

Counting Cells of Order- k Voronoi Tessellations in \mathbb{R}^3 with Morse Theory

Ranita Biswas  

IST Austria (Institute of Science and Technology Austria), Klosterneuburg, Austria

Sebastiano Cultrera di Montesano  

IST Austria (Institute of Science and Technology Austria), Klosterneuburg, Austria

Herbert Edelsbrunner  

IST Austria (Institute of Science and Technology Austria), Klosterneuburg, Austria

Morteza Saghafian  

Department of Mathematical Sciences, Sharif University of Technology, Tehran, Iran

Abstract

Generalizing Lee’s inductive argument for counting the cells of higher order Voronoi tessellations in \mathbb{R}^2 to \mathbb{R}^3 , we get precise relations in terms of Morse theoretic quantities for piecewise constant functions on planar arrangements. Specifically, we prove that for a generic set of $n \geq 5$ points in \mathbb{R}^3 , the number of regions in the order- k Voronoi tessellation is $N_{k-1} - \binom{k}{2}n + n$, for $1 \leq k \leq n - 1$, in which N_{k-1} is the sum of Euler characteristics of these function’s first $k - 1$ sublevel sets. We get similar expressions for the vertices, edges, and polygons of the order- k Voronoi tessellation.

2012 ACM Subject Classification Theory of computation \rightarrow Computational geometry

Keywords and phrases Voronoi tessellations, Delaunay mosaics, arrangements, convex polytopes, Morse theory, counting

Digital Object Identifier 10.4230/LIPIcs.SoCG.2021.16

Funding This project has received funding from the European Research Council (ERC) under the European Union’s Horizon 2020 research and innovation programme, grant no. 788183, from the Wittgenstein Prize, Austrian Science Fund (FWF), grant no. Z 342-N31, and from the DFG Collaborative Research Center TRR 109, “Discretization in Geometry and Dynamics”, Austrian Science Fund (FWF), grant no. I 02979-N35.

1 Introduction

The size of the Voronoi tessellation of n points in \mathbb{R}^d (by which we mean the number of cells of dimension between 0 and d) is reasonably well understood, although there are still open questions. In contrast, little is known about higher order Voronoi tessellations, except in \mathbb{R}^2 , where induction can be used to determine the size; see Lee [6]. The original motivation for the work described in this paper is the extension of the inductive argument beyond 2 dimensions. A result like in \mathbb{R}^2 , where the size depends solely on the number of points, cannot be expected even in \mathbb{R}^3 . Nevertheless, we report precise formulas in terms of elementary Morse theoretic concepts, such as the critical cells of piecewise constant functions on arrangements. This connection opens up the use of topological methods to counting cells and related combinatorial quantities.

Prior work. While Voronoi tessellations go back more than 100 years to the seminal work of Voronoi [10] or earlier, higher order Voronoi tessellations have been introduced only recently, by Shamos and Hoey [8] in computational geometry and by Gábor Fejes Tóth [4] in discrete geometry. Particularly important for this paper is the incremental algorithm of Lee [6], which also serves as inductive counting argument and establishes that the order- k Voronoi



© Ranita Biswas, Sebastiano Cultrera di Montesano, Herbert Edelsbrunner, and Morteza Saghafian;

licensed under Creative Commons License CC-BY 4.0

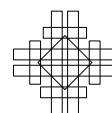
37th International Symposium on Computational Geometry (SoCG 2021).

Editors: Kevin Buchin and Éric Colin de Verdière; Article No. 16; pp. 16:1–16:15

Leibniz International Proceedings in Informatics



Schloss Dagstuhl – Leibniz-Zentrum für Informatik, Dagstuhl Publishing, Germany



tessellation of n points in \mathbb{R}^2 , as defined in Section 2.1, has $\Theta(kn)$ vertices, edges, and regions. This implies that the first k higher order Voronoi tessellations have size $\Theta(k^2n)$. The latter bound was extended to $\Theta(k^{\lceil \frac{d+1}{2} \rceil} n^{\lfloor \frac{d+1}{2} \rfloor})$ in \mathbb{R}^d by Clarkson and Shor [2]. Indeed, it is easy to give tight bounds on the total size, over all orders $1 \leq k \leq n-1$, but there are no good bounds known for individual orders beyond 2 dimensions.

To illustrate the difficulties, we mention that the size of the (order-1) Voronoi tessellation of n points in \mathbb{R}^3 depends not only on n but also on how the points are distributed in space. If the points are uniformly distributed within the unit cube, the expected size is $\Theta(n)$, but if the points are placed on the moment curve, then the size is $\Theta(n^2)$. On the other hand, the total size, over all orders, depends only on n and is therefore the same for both sets. This suggests that for large values of k , the uniformly distributed points have larger Voronoi tessellations than the points on the moment curve, and this has been experimentally quantified in [3].

Results. We extend the inductive approach of Lee [6] to 3 dimensions. The basis of this extension is the contractibility of the skeleta that split the regions for order $k-1$ into the pieces that combine to the regions for order k . Weaker versions of this lemma can be found in Lee [6] for \mathbb{R}^2 and in [3] for \mathbb{R}^d . The inductive approach is simplified by interpreting the tessellations in projective rather than Euclidean space. This effectively combines the order- k and the order- $(n-k)$ tessellations, with the benefit that in 2 dimensions we have precisely $(2k-1)(n-k) - (k-2)$ regions, and similar expressions for the number of edges and vertices, provided the n points be in general position. Similarly, in 3 dimensions we have precisely $N_{k-1} - \binom{k}{2}n + n$ regions, and similar expressions for the number of polygons, edges, and vertices, again with the only requirement that the points be in general position. The N_k form the connection to discrete Morse theory. Specifically, $N_k = M_1 + M_2 + \dots + M_k$, in which M_i is the alternating sum of critical polygons of order at most i in $\binom{n}{2}$ 2-dimensional arrangements of $n-2$ lines each. For n points on the moment curve, each such arrangement has only two critical polygons: one at order $k=1$ and the other at order $k=n-1$. Hence $N_k = k\binom{n}{2}$, for $1 \leq k \leq n-2$, and $N_{n-1} = n\binom{n}{2}$, and we get a complete description of the size but also of the combinatorial structure of the higher order Voronoi tessellations. For the general case, the determination of the N_k is however a difficult question.

Outline. Section 2 explains the background needed to appreciate this paper, which are basic geometric results on Voronoi tessellations, plane arrangements, and convex polytopes. Section 3 extends the inductive argument of Lee [6] to 3 dimensions, getting relations for the number of cells in terms of alternating sums of critical polygons. Section 4 introduces the Morse theoretic framework within which the alternating sums can be interpreted as Euler characteristics of sublevel sets of discrete Morse functions. Section 5 concludes the paper.

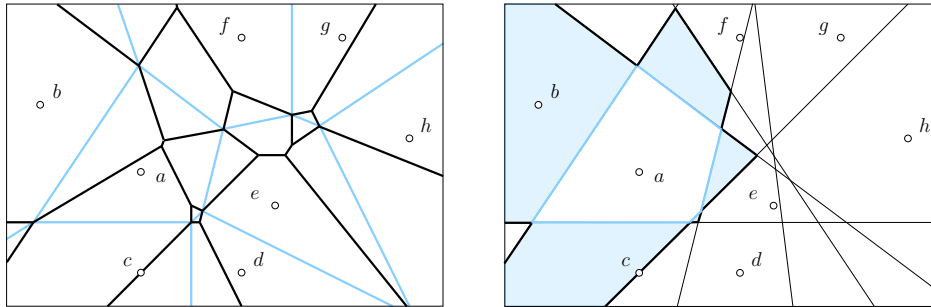
2 Geometric Background

We introduce order- k Voronoi tessellations and k -th Brillouin zones in d dimensions, together with an explanation of the connection to arrangements in $d+1$ dimensions. In addition, we prove that the skeleta along which the regions in the order- k tessellations split are contractible.

2.1 Voronoi Tessellations and Brillouin Zones

Let A be a finite set of points in \mathbb{R}^d and write $n = \#A$ for the cardinality. For any subset $Q \subseteq A$, the *region* of Q is the set of points in \mathbb{R}^d that are at least as close to the points in Q as to the points not in Q . Each such region is a d -dimensional convex polyhedron, and the

common intersection of any collection of regions, each defined by the same number of points, is either empty or a face common to all of them. We follow [6, 8] in defining the *order- k Voronoi tessellation* of A , denoted $\text{Vor}_k(A)$, as the polyhedral complex whose cells are the regions defined by subsets Q of size k together with all their faces; see Figure 1, left panel. By definition, the order-0 tessellation consists of a single region, which is the entire \mathbb{R}^d .



■ **Figure 1** *Left panel:* starting with the blue (order-1) Voronoi tessellation of the points, we construct the order-2 Voronoi tessellation by dividing up the order-1 regions with solid black lines and merging them across the blue lines. *Right panel:* the bisectors of a and all other points divide the plane into the Brillouin zones of a . The highlighted second Brillouin zone is where a expands from the order-1 to the order-2 Voronoi tessellation; compare with left panel.

The set of points in \mathbb{R}^d for which $a \in A$ is the k -th nearest is the k -th Brillouin zone of a . As illustrated in the right panel in Figure 1, this set consists of a number of regions in the arrangement formed by the bisectors of a and the other points in A . The first Brillouin zone is a convex polyhedron, and each of the other zones has the homotopy type of a sphere. Furthermore, the union of the first k zones is star-convex, with a in the kernel; see [4]. Importantly, for $k \geq 2$, every region in the k -th Brillouin zone is a d -dimensional convex polytope whose boundary can be partitioned into the *near boundary*, which is visible from a , the *far boundary*, which is not visible from a , and the *silhouette*, which separates the near and far boundaries. By convexity, the silhouette is homeomorphic to a $(d - 2)$ -sphere that splits the boundary into two pieces, each homeomorphic to an open $(d - 1)$ -ball.

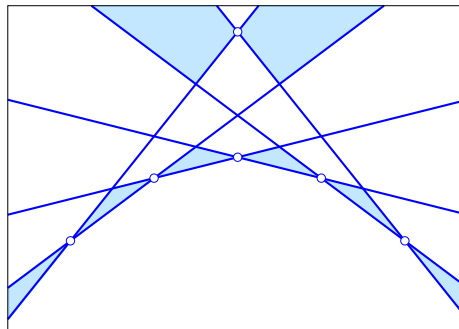
2.2 Plane Arrangement

It is useful to consider the collection of d -dimensional planes in \mathbb{R}^{d+1} obtained by mapping each point $a \in A$ to the affine function $\alpha: \mathbb{R}^d \rightarrow \mathbb{R}$ defined by $\alpha(x) = 2\langle x, a \rangle - \|a\|^2$. Note that α encodes the squared Euclidean distance from a : $\|x - a\|^2 = \|x\|^2 - \alpha(x)$. The graph of α is a (non-vertical) d -plane in \mathbb{R}^{d+1} . The collection of d -planes decomposes \mathbb{R}^{d+1} into convex cells of dimension $0 \leq i \leq d + 1$, referred to as the *arrangement* of d -planes. We call the $(d + 1)$ -cells *chambers*, and the d -cells *facets*. For $1 \leq k \leq n$, the k -th level of the arrangement is the set of points $(x, y) \in \mathbb{R}^d \times \mathbb{R}$ such that $\alpha(x) < y$ for at most $k - 1$ affine maps and $\alpha(x) > y$ for at most $n - k$ affine maps. The k -th belt is the set of points between the k -th level and the $(k + 1)$ -st level.

► **Lemma 2.1** (From Arrangement to Tessellation). *Let A be a set of n points in \mathbb{R}^d , let $0 \leq k \leq n$, and recall that A defines an arrangement of n non-vertical d -planes in \mathbb{R}^{d+1} .*

- *There is a bijection between the regions of $\text{Vor}_k(A)$ and the chambers of the k -th belt such that each region is the vertical projection of the corresponding chamber.*
- *The k -th Brillouin zone of $a \in A$ is the vertical projection of the k -th level intersected with the d -plane defined by a .*

As illustrated in Figure 2, it is convenient to take the projective view, in which we connect the levels and belts at infinity. Henceforth, this is what we mean by the k -th belt, namely the (non-projective) k -th and $(n - k)$ -th belts connected at infinity, and similarly for the Voronoi tessellations, and the Brillouin zones. Figure 1 shows the non-projective concepts, and to make them projective, we would add the overlay of the order-7 and the order-6 to the left panel, and we would shade the wedge on the lower right in the right panel since it belongs to the shaded region that contains b on the left. Note that the k -th belt is the same as the $(n - k)$ -th belt, for every k . Counting every cell twice, this amounts to a double-covering of the d -dimensional projective space. The main reason for adapting this view is the resulting simplification of the counting arguments and the beautification of the results.



■ **Figure 2** The first belt in the projective line arrangement consists of all chambers above exactly one line and all chambers below exactly one line. The unbounded chambers are paired up, and each pair is considered a single chamber. We thus count 6 (light blue) chambers in the first belt.

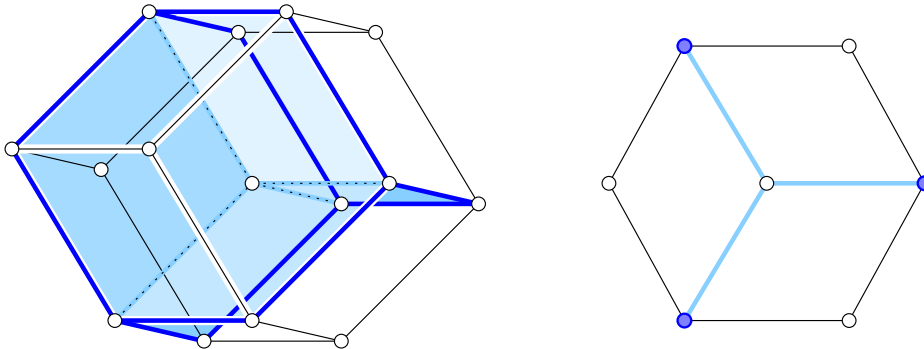
Another useful because simplifying assumption is that the points be in *general position*, by which we mean that any i -dimensional plane in \mathbb{R}^d passes through at most $i + 1$ points, and any i -dimensional sphere passes through at most $i + 2$ points of A , for $0 \leq i \leq d - 1$. If the points are in general position, the corresponding arrangement of d -planes in \mathbb{R}^{d+1} is generic; that is: any $i + 1$ d -planes intersect in a $(d - i)$ -dimensional plane. This implies that any $d + 2$ or more d -planes have an empty common intersection.

2.3 Convex Polytopes and Their Skeleta

Consider $n \geq d + 2$ points in general position in \mathbb{R}^d . In the projective view, every chamber in the corresponding arrangement in \mathbb{R}^{d+1} is a (bounded) convex $(d + 1)$ -polytope, and in the doubly-covered view, there is a second, *antipodal* copy of the polytope in the arrangement. The boundary of the chamber consists of i -dimensional cells, for $0 \leq i \leq d$, each a (convex) i -polytope itself. Because of general position, the chamber is *simple*, by which we mean that every vertex belongs to $d + 1$ facets, every edge belongs to d facets, etc. It follows that every vertex belongs to $d + 1$ edges, which we express by saying that the vertex has *degree* $d + 1$.

By Lemma 2.1, every region in the order- k Voronoi tessellation is the vertical projection of a chamber, and by construction, the projection is *generic*, in the sense that its restriction preserves the dimension of every face in the boundary. Since the projection is in the vertical direction, it makes sense to distinguish between *lower* and *upper facets*. The k -th belt consists of chambers above k planes or below k planes, and to be consistent, we reverse upper/lower for the latter type. This will not cause any confusion since we always look at a single chamber, which we may assume is bounded and of the former type. The *lower boundary* of

such a chamber consists of all lower facets and their faces, the *upper boundary* consists of all upper facets and their faces, and the *silhouette* is the intersection of the lower and the upper boundaries. The projection of the silhouette is the boundary of the projected chamber. Although this is a generic projection of a simple $(d + 1)$ -polytope, it is not necessarily a simple d -polytope. Indeed, a vertex of the silhouette may be incident to i lower facets and $j = d + 1 - i$ upper facets, for any $1 \leq i \leq d$. Such a vertex belongs to ij $(d - 1)$ -cells in the silhouette. See the dodecahedron in Figure 3 as an example, which has 8 degree-3 vertices and 6 degree-4 vertices.



■ **Figure 3** *Left:* projecting the 4-cube along a diagonal gives the rhombic dodecahedron in \mathbb{R}^3 , which we see decomposed into four distorted 3-cubes. The projection of the silhouette is the boundary of the dodecahedron. The projection of the upper 2-skeleton of the 4-cube consists of the vertices, edges, and *light blue* polygons shared by the distorted 3-cubes. Its boundary is a graph in the boundary of the dodecahedron, which we highlight with *dark blue* edges. *Right:* the analogous construction one dimension lower, in which the 3-cube projects to a decomposed hexagon.

We call the cells of dimension less than d in the lower boundary minus the silhouette the *lower skeleton* of the chamber. Symmetrically, we define the *upper skeleton* of the chamber. Both skeleta are open and $(d - 1)$ -dimensional. The *boundary* of the lower skeleton consists of all proper faces of its $(d - 1)$ -cells that belong to the silhouette, and similarly for the upper skeleton. Adding their boundaries, we get the *closed lower* and *upper skeleta*. For example, the blue open trigon in the projection of the 3-cube in Figure 3 is the upper skeleton, and closed trigon is the closed upper skeleton. We will make heavy use of a topological property of the closed skeleta that does not hold for general convex polyhedra and therefore also not for chambers in general arrangements.

► **Lemma 2.2 (Contractible Skeleta).** *Let A be a set of $n \geq d + 2$ points in general position in \mathbb{R}^d , let $1 \leq k \leq n - 1$, and consider a chamber in the k -th belt of the corresponding arrangement in \mathbb{R}^{d+1} . Then the closed lower skeleton of this chamber is contractible unless $k = 1$, and the closed upper skeleton is contractible, unless $k = n - 1$. In the two exceptional cases, the skeleta are empty.*

Proof. We consider the lower skeleton first. Let $Q \subseteq A$ with $\#Q = k$ such that the projection of the chamber to \mathbb{R}^d is the region of points that satisfy $\|x - a\| \leq \|x - b\|$ for all $a \in Q$ and all $b \in A \setminus Q$. We denote this region R , and for each $a \in Q$, we write $R_a \subseteq R$ for the subset of points for which a is the k -th nearest or, equivalently, the furthest of the points in Q . We note that R_a is convex and indeed a region of the k -th Brillouin zone of a . Assuming $k \geq 2$, the boundary of R_a can be partitioned into the near boundary, which is visible from a , the far boundary, which is not visible from a , and the silhouette, which separates the two.

Indeed, the projection of the closed lower skeleton is the union of the near boundaries of all R_a , with $a \in Q$. To prove that the closed lower skeleton is contractible, we give an explicit deformation retraction from R to the projection of the closed lower skeleton. Within R_a , the deformation retraction moves every point $x \in R_a$ straight toward a until it reaches the near boundary of R_a . This is well defined because $k \geq 2$ so that a lies outside R_a . Because R is convex and therefore contractible, the existence of this deformation retraction implies that the lower skeleton is contractible.

We consider the upper skeleton second. For each $b \in A \setminus Q$, we write $R_b \subseteq R$ for the subset of points for which b is the $(k + 1)$ -st nearest or, equivalently, the nearest of the points in $A \setminus Q$. Now the near boundary of R_b belongs to the boundary of R , and the projection of the closed upper skeleton is the union of far boundaries of all R_b , with $b \in A \setminus Q$. Like before, the deformation retraction moves a point $y \in R_b$ straight away from b until it hits the far boundary of R_b . This construction works for $k \leq n - 2$, as claimed. ◀

For the cases in which Lemma 2.2 guarantees contractibility, we will refer to the closed skeleta as *closed $(d - 1)$ -trees* and their open versions simply as *$(d - 1)$ -trees*.

3 Counting in Three Dimensions

We count the cells of the Voronoi tessellations in 3 dimensions inductively, following the pattern of the 2-dimensional argument pioneered by Lee [6]. To begin, we need some understanding of 4-dimensional convex polytopes and their projections.

3.1 Chambers Projected to Regions

It is instructive to look at the 4-cube and its projection along a diagonal direction, which is known as the *rhombic dodecahedron*; see Figure 3. Each endpoint of the diagonal is incident to four 3-cubes in the boundary, and their projections form two decompositions of the rhombic dodecahedron into four distorted 3-cubes each. While the 4-cube is simple and the projection is generic, the rhombic dodecahedron is not simple: it has vertices of degree 3 and of degree 4. The two decompositions into distorted 3-cubes are by projecting the lower skeleton and the upper skeleton of the 4-cube, which by Lemma 2.2 are 2-trees. The boundary of each 2-tree is a graph in the silhouette of the 4-cube. Figure 3 shows one of these graphs, which connects some of the degree-3 vertices and all of the degree-4 vertices by dark blue edges. The other graph (not shown) uses the remaining edges in the silhouette. The two graphs are disjoint except that they share all degree-4 vertices, where they cross. This is a pattern that can be observed in general and not just in the example depicted in Figure 3.

We use the combinatorics of the 2-trees to count the cells in the order- k Voronoi tessellation, which we recall are obtained by projecting the chambers in the k -th belt of the arrangement in \mathbb{R}^4 . It will be important to count the cells of different dimension and of different type separately. We thus use the following notation:

$$u_k = \# \text{old vertices}, \quad v_k = \# \text{mid vertices}, \quad w_k = \# \text{new vertices}, \tag{1}$$

$$d_k = \# \text{old edges}, \quad e_k = \# \text{new edges}, \tag{2}$$

$$p_k = \# \text{polygons}, \quad r_k = \# \text{regions}, \tag{3}$$

in which we call a vertex *old*, *mid*, or *new* in the order- k Voronoi tessellation if it belongs to the tessellations of orders $k - 2, k - 1, k$, orders $k - 1, k, k + 1$, or orders $k, k + 1, k + 2$. Similarly, we call an edge *old* or *new* in the order- k Voronoi tessellation if it belongs to the tessellations of orders $k - 1, k$ or orders $k, k + 1$.

3.2 Graphs and 2-Trees

Recall that the upper 2-tree of a chamber contains all vertices, edges, and polygons shared by at least two of the upper facets. This implies that the boundary of this 2-tree consists of the new edges and the mid and new vertices in the silhouette. Symmetrically, the boundary of the lower 2-tree consists of the old edges and the mid and old vertices in the silhouette. Together, the two graphs exhaust all edges and vertices, and they intersect in the mid vertices, where they cross. We call a cycle in the graph a *loop* and the cyclomatic number the *number of loops*, which for a connected graph is $\#\text{edges} - \#\text{vertices} + 1$. Let u, v, w, d, e be the numbers of old, mid, new vertices and old, new edges in the silhouette.

► **Lemma 3.1** (Loops in Graphs). *The boundary of the upper 2-tree is a connected graph with $\frac{1}{2}w + 1$ loops, and the boundary of the lower 2-tree is a connected graph with $\frac{1}{2}u + 1$ loops.*

Proof. It suffices to consider the boundary of the upper 2-tree. It is connected, else the 2-tree would not be contractible. It has e edges, v vertices of degree 2, and w vertices of degree 3, which implies $2e = 2v + 3w$. The number of loops is $e - (v + w) + 1 = \frac{1}{2}w + 1$. ◀

The combinatorics of the boundary is important for the combinatorics of the 2-tree, but it does not determine it. We therefore introduce a shape variable, which together with the graph determines the number of vertices, edges, and polygons in the 2-tree. The corresponding intuition will be revealed in Section 4.1. We call a polygon a *minimum* if its entire boundary belongs to the 2-tree. Otherwise, the part of the boundary in the 2-tree consists of $\mu + 1$ arcs, and we call the polygon a *maximum* if $\mu = -1$, a *non-critical polygon* if $\mu = 0$, and a *saddle* with *multiplicity* μ if $\mu \geq 1$. The shape variable of the polygon is $\#\text{edges} - \#\text{vertices} + 1$, in which we count only the faces in the 2-tree. Note that this is 1 for a minimum and maximum, 0 for a non-critical polygon, and $-\mu$ for a saddle with multiplicity μ . Taking the sum over the polygons in the upper 2-tree, we get the *characteristic* of the chamber, which we denote J . It is also defined for 2-skeleta that are not contractible, but the relation expressed in the next lemma holds only for 2-trees.

► **Lemma 3.2** (Size of 2-Tree). *Let A be a set of n points in general position in \mathbb{R}^3 and $1 \leq k \leq n - 1$. The numbers of vertices, edges, and polygons in the upper 2-tree of a chamber in the k -th belt satisfy*

$$W = \frac{1}{2}w - 1 + J, \tag{4}$$

$$E = \frac{3}{2}w - 2 + 2J, \tag{5}$$

$$P = \frac{3}{2}w + J, \tag{6}$$

in which w is the number of new vertices in the silhouette, and J is the characteristic of the chamber.

Proof. We first dispose of an easy case: when the 2-tree contains a maximum. Then $J = 1$ because the 2-tree contains only this one polygon and has no edges and no vertices. Furthermore, $w = 0$, so the claimed relations give $W = 0$, $E = 0$, $P = 1$, as required.

We can therefore assume that the 2-tree contains no maximum, but there may be minima and saddles beside the non-critical polygons. Consider the graph formed by the edges and vertices in the 2-tree, to which we add the w new vertices in the silhouette so that each edge has both endpoints. For each minimum in the 2-tree, this graph contains a loop, and for each saddle with multiplicity μ , the graph contains μ extra components. The characteristic is $J = \#\text{loops} - \#\text{components} + 1$, and the number of edges is

$$E = W + w + \#\text{loops} - \#\text{components} = W + w - 1 + J. \tag{7}$$

16:8 Counting Cells of Order- k Voronoi Tessellations in \mathbb{R}^3 with Morse Theory

We also have $2E = 4W + w$, which combined with (7) implies (4) and (5). To prove (6), we recall that the closed 2-tree is contractible, which implies that its Euler characteristic satisfies $(W - E + P) + (v + w - e) = 1$. Substituting $E = 2W + \frac{1}{2}w$ and $e = v + \frac{3}{2}w$ implies $P = W + w + 1 = \frac{3}{2}w + J$, as required. \blacktriangleleft

For counting purposes, we write J_{k+1} for the sum of characteristics of the chambers in the k -th belt, for $0 \leq k \leq n - 1$. By Lemma 2.2, the upper 2-skeleton of every chamber is contractible and therefore a 2-tree for $1 \leq k \leq n - 2$. For $k = 0$, there is a single chamber whose upper boundary projects to the entire first Voronoi tessellation. Its upper 2-skeleton is therefore not a 2-tree, but its characteristics is still defined, namely the number of polygons in $\text{Vor}_1(A)$.

3.3 Induction

We count the vertices, edges, polygons, and regions of the Voronoi tessellations inductively, beginning with order $k = 1$.

► **Lemma 3.3** (Induction Basis in \mathbb{R}^3). *The order-1 Voronoi tessellation of $n \geq 5$ points in general position in \mathbb{R}^3 has*

$$w_1 = J_1 - n \text{ vertices}, \quad (8)$$

$$e_1 = 2J_1 - 2n \text{ edges}, \quad (9)$$

$$p_1 = J_1 \text{ polygons}, \quad (10)$$

$$r_1 = n \text{ regions}. \quad (11)$$

Proof. We have $p_1 = J_1$ by definition, and $r_1 = n$ because the order-1 Voronoi tessellation has one region for each point. To get the relations for the vertices and edges, we note that the order-1 Voronoi tessellation is a polyhedral complex that decomposes the 3-sphere, so that Euler's formula implies $w_1 - e_1 + p_1 - r_1 = 0$. By assumption of general position, every vertex belongs to 4 edges, which gives $4w_1 - 2e_1 = 0$. Combining these two relations, we can express w_1 and e_1 in terms of p_1 and r_1 and therefore in terms of J_1 and n , as stated. \blacktriangleleft

When we go from the order- $(k - 1)$ to the order- k Voronoi tessellation, we see some cells die, some cells age, and some cells get born according to relations (4), (5), (6).

► **Lemma 3.4** (Induction Step in \mathbb{R}^3). *The numbers of old, mid, new vertices, old and new edges, polygons, and regions of the order- k Voronoi tessellation of n points in general position in \mathbb{R}^3 satisfy*

$$u_k = v_{k-1}, \quad (12)$$

$$v_k = w_{k-1}, \quad (13)$$

$$w_k = 2w_{k-1} - r_{k-1} + J_k, \quad (14)$$

$$d_k = e_{k-1}, \quad (15)$$

$$e_k = 6w_{k-1} - 2r_{k-1} + 2J_k, \quad (16)$$

$$p_k = 6w_{k-1} + J_k, \quad (17)$$

$$r_k = w_{k-1} - v_{k-1} + r_{k-1}, \quad (18)$$

for $2 \leq k \leq n - 1$.

Proof. Rules (12), (13), (15) express aging. By assumption of general position, each new vertex of $\text{Vor}_{k-1}(A)$ belongs to four regions, so we get rule (14) from (4), rule (16) from (5), and rule (17) from (6). To get rule (18), we note that each of the $u_k + w_k$ old and new vertices has degree 4, and each of the v_k mid vertices has degree 8, again by assumption of general position. Hence $2(d_k + e_k) = 4(u_k + 2v_k + w_k)$. Plugging this into the Euler formula for the 3-sphere, we get $r_k = (u_k + v_k + w_k) - (d_k + e_k) + p_k = p_k - (u_k + 3v_k + w_k)$, which implies (18). ◀

These rules can be used to find expressions for the cells in the Voronoi tessellations. Recall that J_k is the alternating sum of critical polygons of order k ; see text following the proof of Lemma 3.2. It will be convenient to write $M_k = J_1 + J_2 + \dots + J_k$ and $N_k = M_1 + M_2 + \dots + M_k = kJ_1 + (k - 1)J_2 + \dots + J_k$, and to set $J_k = M_k = N_k = 0$ for $k \leq 0$.

► **Theorem 3.5** (Size of Order- k Voronoi Tessellations in \mathbb{R}^3). *For $1 \leq k \leq n - 1$, the order- k Voronoi tessellation of $n \geq 5$ points in \mathbb{R}^3 has*

$$u_k \leq N_{k-2} - \binom{k-1}{2}n \text{ old vertices,} \tag{19}$$

$$v_k \leq N_{k-1} - \binom{k}{2}n \text{ mid vertices,} \tag{20}$$

$$w_k \leq N_k - \binom{k+1}{2}n \text{ new vertices,} \tag{21}$$

$$d_k \leq 2N_{k-1} + 2N_{k-2} - 2(k - 1)^2n \text{ old edges,} \tag{22}$$

$$e_k \leq 2N_k + 2N_{k-1} - 2k^2n \text{ new edges,} \tag{23}$$

$$p_k \leq 6N_{k-1} + J_k - 6\binom{k}{2}n \text{ polygons,} \tag{24}$$

$$r_k \leq N_{k-1} - \binom{k}{2}n + n \text{ regions,} \tag{25}$$

with equality in all seven cases if the points are in general position.

Proof. Let A be a set of $n \geq 5$ points in \mathbb{R}^3 . Whenever A is not in general position, we can perturb it into general position without losing any vertex, edge, polygon, or region in any of its Voronoi tessellations. We can therefore assume without loss of generality that A is in general position and prove that in this case the seven claimed inequalities are equations.

For $k = 1$, we have $u_1 = v_1 = 0$, $w_1 = J_1 - n$, $d_1 = 0$, $e_1 = 2J_1 - 2n$, $p_1 = J_1$, and $r_1 = n$, which agrees with Lemma 3.3. Assuming the relations are correct for index $k - 1$, we use Lemma 3.4 to prove that they are correct for k . (19), (20), (22) follow straightforwardly from (12), (13), (15) and (21), (23). To see (21), (23), (24), (25), we use (14), (16), (17), (18) to compute

$$w_k = [2N_{k-1} - N_{k-2} + J_k] - [2\binom{k}{2} - \binom{k-1}{2} + 1]n = N_k - \binom{k+1}{2}n, \tag{26}$$

$$e_k = [6N_{k-1} - 2N_{k-2} + 2J_k] - [6\binom{k}{2} - 2\binom{k-1}{2} + 2]n = 2N_k + 2N_{k-1} - 2k^2n, \tag{27}$$

$$p_k = [6N_{k-1} + J_k] - 6\binom{k}{2}n, \tag{28}$$

$$r_k = [N_{k-1} - N_{k-2} + N_{k-2}] - [\binom{k}{2} - \binom{k-1}{2} + \binom{k-1}{2} - 1]n = N_{k-1} - \binom{k}{2}n + n, \tag{29}$$

as claimed. ◀

3.4 Relations of Symmetry

By projective interpretation, the order- k Voronoi tessellation is also the order- $(n - k)$ Voronoi tessellation. Indeed, the only difference between the two is that upper and lower facets switch, and so do old and new vertices and old and new edges. We state these relations formally and use them to derive a similar relation for the characteristics of the belts.

16:10 Counting Cells of Order- k Voronoi Tessellations in \mathbb{R}^3 with Morse Theory

► **Theorem 3.6** (Symmetry Relations). *The numbers of old, mid, new vertices, old and new edges, polygons, regions, and the characteristics of the order- k Voronoi tessellations of $n \geq 5$ points in general position in \mathbb{R}^3 satisfy $u_k = w_{n-k}$, $v_k = v_{n-k}$, $w_k = u_{n-k}$, $d_k = e_{n-k}$, $e_k = d_{n-k}$, $p_k = p_{n-k}$, $r_k = r_{n-k}$, $J_k = J_{n-k}$, for $1 \leq k \leq n-1$.*

Proof. The symmetry relations for the vertices, edges, polygons, and regions follow from the symmetry of the projective definition of order- k Voronoi tessellations. To see the relation for the characteristic, we note that $\binom{k+1}{2} - 2\binom{k}{2} + \binom{k-1}{2} = 1$ and that $N_k - 2N_{k-1} + N_{k-2} = M_k - M_{k-1} = J_k$, for $1 \leq k \leq n-1$. Using $r_k = N_{k-1} - \binom{k}{2}n + n$ from Theorem 3.5 and the symmetry relation for the regions, we get

$$0 = [r_{k+1} - 2r_k + r_{k-1}] - [r_{n-k-1} - 2r_{n-k} + r_{n-k+1}] = [J_k - n] - [J_{n-k} - n]. \quad (30)$$

Simplifying (30), we get the claimed symmetry relation for the characteristic. ◀

To provide examples, we list the number of cells and characteristics of belts for two sets of six points each in Table 1. Observe the symmetry in the columns as predicted by Theorem 3.6, and note that the numbers given for the moment curve example are consistent with the expressions given in Section 1.

■ **Table 1** Numbers of vertices, edges, polygons, and regions for six points on the moment curve in \mathbb{R}^3 in the *upper table*, and of the six points of the double suspended tetrahedron in the *lower table*.

k	u_k	v_k	w_k	d_k	e_k	p_k	r_k	J_k	M_k	N_k
1	0	0	9	0	18	15	6	15	15	15
2	0	9	12	18	42	54	15	0	15	30
3	9	12	9	42	42	72	18	0	15	45
4	12	9	0	42	18	54	15	0	15	60
5	9	0	0	18	0	15	6	15	30	90
Σ	30	30	30	120	120	210	60	30	90	240
1	0	0	8	0	16	14	6	14	14	14
2	0	8	14	16	44	52	14	4	18	32
3	8	14	8	44	44	78	20	-6	12	44
4	14	8	0	44	16	52	14	4	16	60
5	8	0	0	16	0	14	6	14	30	90
Σ	30	30	30	120	120	210	60	30	90	240

4 A Morse Theoretic Perspective

The J_k, M_k, N_k have alternative interpretations in terms of sublevel sets of discrete Morse functions. As we will see, these functions are closer in spirit to the discrete Morse theory introduced by Banchoff [1] than the more popular version developed by Forman [5]. It is convenient to adopt the language of great-circle arrangements in the sphere instead of doubly-covered projective line arrangements in the plane, which are of course equivalent.

4.1 Arrangements of Great-Circles

Let A be a set of n points in general position, let a, b, c be three different points in A , and recall that they correspond to affine functions $\alpha, \beta, \gamma: \mathbb{R}^3 \rightarrow \mathbb{R}$. We are interested in $\alpha(x) = \beta(x)$, which describes a plane in \mathbb{R}^3 , in $\gamma(x) = \alpha(x) = \beta(x)$, which describes a line, and in $\gamma(x) \leq \alpha(x) = \beta(x)$, which describes a half-plane; see Figure 4. In our spherical view, the plane becomes a sphere, denoted $S_{a,b}$, and for each point c , we get a hemi-sphere,

$H_c \subseteq S_{a,b}$. The $n - 2$ lines decomposing the plane correspond to the same number of great-circles that decompose the sphere into vertices, edges, and (spherical) polygons, which appear in antipodal pairs. The main concept in this section is the function

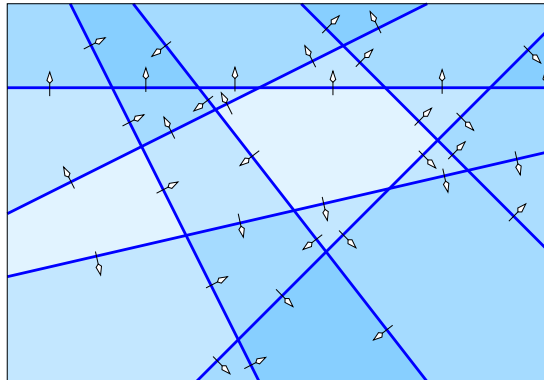
$$f_{a,b}(\varphi) = 1 + \#\{c \in A \setminus \{a, b\} \mid \varphi \subseteq H_c\}, \tag{31}$$

in which φ is a polygon in the great-circle arrangement on $S_{a,b}$. For completeness, we define $f_{a,b}$ for an edge or a vertex equal to the smallest value of any polygon incident to the edge or vertex. Write $\bar{\varphi}$ for the antipodal polygon of φ , and call a polygon, ψ , a *neighbor* of φ if the two share an edge. Then we have

$$f_{a,b}(\varphi) = f_{a,b}(\psi) \pm 1, \tag{32}$$

$$f_{a,b}(\varphi) = n - f_{a,b}(\bar{\varphi}), \tag{33}$$

for all neighbors ψ of φ . We get (32) by assumption of general position, and (33) by symmetry. Consistent with Section 3, we call φ a *minimum* if $f_{a,b}(\varphi) = f_{a,b}(\psi) - 1$ and a *maximum*



■ **Figure 4** An arrangement of lines in which the shading indicates the coverage with half-planes. The arrows go from smaller to larger coverage. Considering only polygons that are fully contained inside the box, we see one minimum, one simple saddle, and seven non-critical polygons.

if $f_{a,b}(\varphi) = f_{a,b}(\psi) + 1$ for all neighbors ψ of φ . Otherwise, the function values of the cyclically ordered neighbors change $2(\mu + 1) \geq 2$ times between $f_{a,b}(\varphi) \pm 1$. For $\mu = 0$, φ is a *non-critical polygon*, and for $\mu \geq 1$, it is a *saddle with multiplicity μ* .

4.2 Sublevel Sets and Euler Characteristics

A common feature in Morse theoretic studies is the occurrence of sublevel sets and their relations. For each k , the sublevel set $f_{a,b}^{-1}(-\infty, k]$ is a closed subset of $S_{a,b}$, with well-defined *Betti numbers*, $\beta_p(k)$, and *Euler characteristic*, $\chi(k) = \beta_0(k) - \beta_1(k) + \beta_2(k)$. Define $\text{index}(\varphi) = 0, 1, 2$ if φ is a minimum, saddle, maximum. In the discrete setting at hand, it is not difficult to prove an analog of the Euler–Poincaré Theorem, which implies that $\chi(k)$ is the sum of $(-1)^{\text{index}(\varphi)}$, over all critical polygons that satisfy $f_{a,b}(\varphi) \leq k$, in which a saddle with multiplicity μ is counted as μ simple saddles. We define $J_k(a, b) = \chi(k) - \chi(k - 1)$, $M_k(a, b) = \chi(k)$, and $N_k(a, b) = \chi(1) + \chi(2) + \dots + \chi(k)$. The connection to the previous discussion and, in particular, Theorem 3.5 should be clear, namely

$$J_k = \sum_{a,b \in A} J_k(a, b), \quad (34)$$

$$M_k = \sum_{a,b \in A} M_k(a, b), \quad (35)$$

$$N_k = \sum_{a,b \in A} N_k(a, b), \quad (36)$$

in which the sums are over all unordered pairs in A . In other words, we have a piecewise constant function on the disjoint union of $\binom{n}{2}$ spheres, $f: \mathbb{S}^2 \sqcup \mathbb{S}^2 \sqcup \dots \sqcup \mathbb{S}^2 \rightarrow [1, n-1]$, whose components are the functions $f_{a,b}$, such that M_k is the Euler characteristic of $f^{-1}(-\infty, k]$, and J_k is the increment from $k-1$ to k . Equivalently, J_k is the alternating sum of critical polygons in $f^{-1}(k)$. We note that this interpretation implies a strengthening of the relation $J_k = J_{n-k}$ in Theorem 3.6: $J_k(a, b) = J_{n-k}(a, b)$, for all pairs $a \neq b$, because antipodal polygons have the same contribution to the sum.

4.3 Relations for Sums

Observe that a generic arrangement of n 3-dimensional great-spheres in \mathbb{S}^4 has $2\binom{n}{4}$ vertices, $8\binom{n}{4}$ edges, $12\binom{n}{4} + 2\binom{n}{2}$ polygons, $8\binom{n}{4} + 4\binom{n}{2}$ facets, and $2\binom{n}{4} + 2\binom{n}{2} + 2$ chambers. This implies relations on the number of cells in the Voronoi tessellations.

► **Theorem 4.1** (Sum Relations). *The new vertices, new edges, polygons, and regions of the Voronoi tessellations of $n \geq 5$ points in general position in \mathbb{R}^3 satisfy*

$$\sum_{k=1}^{n-1} w_k = 2\binom{n}{4}, \quad (37)$$

$$\sum_{k=1}^{n-1} e_k = 8\binom{n}{4}, \quad (38)$$

$$\sum_{k=1}^{n-1} p_k = 12\binom{n}{4} + 2\binom{n}{2}, \quad (39)$$

$$\sum_{k=1}^{n-1} r_k = 2\binom{n}{4} + 2\binom{n}{2}. \quad (40)$$

Similarly, the characteristics of the belts, their cumulative sums, and the cumulative sums of those satisfy

$$\sum_{k=1}^{n-1} J_k = 2\binom{n}{2}, \quad (41)$$

$$\sum_{k=1}^{n-1} M_k = n\binom{n}{2}, \quad (42)$$

$$\sum_{k=1}^{n-1} N_k = \left[\binom{n}{2} + 1\right] \binom{n}{2}. \quad (43)$$

Proof. The new vertices, new edges, polygons, and regions of the order- k Voronoi tessellations, for $1 \leq k \leq n-1$, are in bijection with the vertices, edges, polygons, and chambers of the arrangement in \mathbb{S}^4 . Exceptions are the chamber below and above all great-spheres, which are not covered by the tessellations. This implies (37), (38), (39), (40).

We get (41) because the sum of the J_k is equal to the sum of the Euler characteristics of $\binom{n}{2}$ 2-spheres. To see (42), we note that for a pair of antipodal critical polygons, we have $[n - f(\varphi)] + [n - f(\bar{\varphi})] = n$ because $f(\varphi) + f(\bar{\varphi}) = n$ by (33). The contribution of the pair to the sum of the M_k is therefore n if $\varphi, \bar{\varphi}$ are a minimum and a maximum, and $-\mu n$ if $\varphi, \bar{\varphi}$ are saddles with multiplicity μ . The contributions cancel, except for one minimum/maximum pair per 2-sphere, and since there are $\binom{n}{2}$ 2-spheres, the sum of the M_k is $n\binom{n}{2}$. To prove (43), we use (40) and (25), which for points in general position is an equality:

$$\sum_{k=1}^{n-1} N_{k-1} = \sum_{k=1}^{n-1} r_k + n \sum_{k=1}^{n-1} \binom{k}{2} - n \sum_{k=1}^{n-1} 1 = 2\binom{n}{4} + n\binom{n}{3}. \quad (44)$$

By index transformation, the left-hand side is $\sum_{k=1}^{n-2} N_k$, and by straightforward calculations, the right-hand side is $\binom{n}{2} \binom{n-1}{2}$. Adding $N_{n-1} = n \binom{n}{2}$ from (42) on both sides implies the claimed relation. ◀

Observe that the relations in Theorem 4.1 are consistent with the column sums in Table 1, which are the same for the two sets of six points each.

4.4 Relation for Individual Sphere

The proofs of (41) and (42) show that each sphere contributes the same amount, namely 2 to $\sum J_k$ and n to $\sum M_k$. The proof of (43) does not show the same for $\sum N_k$, but it is still true, that is: each sphere contributes the same amount to the sum of the N_k .

► **Theorem 4.2 (Stronger Sum Relation).** *Let A be a set of $n \geq 5$ points in general position in \mathbb{R}^3 . Then $\sum_{k=1}^{n-1} N_k(a, b) = 1 + \binom{n}{2}$ for any two points $a \neq b$ in A .*

Proof. Fix $a, b \in A$ and consider the arrangement of $n - 2$ great-circles on $S_{a,b}$. For convenience, we write J_k, M_k, N_k , and f for $J_k(a, b), M_k(a, b), N_k(a, b)$, and $f_{a,b}$ throughout this proof. The goal is to show $\sum_{k=1}^{n-1} N_k = 1 + \binom{n}{2}$, but we already have $N_{n-1} = n$ from (42) and $N_{n-2} = N_{n-1} - M_{n-1} = n - 2$ from (41) and (42). Indeed, the proofs of (41) and (42) imply the stronger relations for individual spheres. Therefore it suffices to prove

$$X = \sum_{k=1}^{n-3} N_k = 1 + \binom{n}{2} - n - (n - 2) = \binom{n-2}{2}. \tag{45}$$

We rewrite the sum in terms of the J_k . A polygon contributes to J_k only if $f(\psi) = k$, and this contribution depends on the cyclic sequence of neighboring polygons. Distinguishing between polygons φ with $f(\varphi) = k \pm 1$, the contribution to J_k is 1 minus half the number of alternations between these two types along the cycle. We therefore write $J_k = p_k - \frac{1}{2}t_k$, in which p_k is the number of polygons $\psi \subseteq S_{a,b}$ with $f(\psi) = k$, and t_k is the number of triplets of polygons (φ, ψ, ϱ) with $f(\varphi) + 1 = f(\psi) = f(\varrho) - 1 = k$ that share a common vertex. This vertex is where the type of neighboring polygons changes. We call such an ordered triplet of polygons a *short increasing path*. Using $N_k = kJ_1 + (k - 1)J_2 + \dots + J_k$, we get

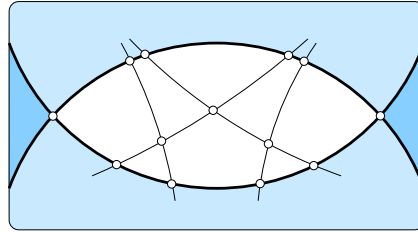
$$X = N_1 + N_2 + \dots + N_{n-3} \tag{46}$$

$$= \binom{n-2}{2}J_1 + \binom{n-3}{2}J_2 + \dots + \binom{2}{2}J_{n-3} \tag{47}$$

$$= \sum_{k=1}^{n-3} \binom{n-k-1}{2}p_k - \frac{1}{2} \sum_{k=1}^{n-3} \binom{n-k-1}{2}t_k. \tag{48}$$

Write Y and Z for the two sums in (48) so that $X = Y - \frac{1}{2}Z$. Observe that Y is the number of triplets (ψ, H, H') , in which ψ is a polygon and $H \neq H'$ are two hemi-spheres that both do not contain ψ . Indeed, if $f(\psi) = k$, then there are $(n - 2) - (k - 1) = n - k - 1$ hemi-spheres that do not contain ψ . Similarly, Z is the number of triplets $((\varphi, \psi, \varrho), H, H')$, in which (φ, ψ, ϱ) is a short increasing path and $H \neq H'$ are two hemi-spheres that both do not contain ψ . We call (ψ, H, H') a *captured polygon* and $((\varphi, \psi, \varrho), H, H')$ a *captured short increasing path*. In words, $X = Y - \frac{1}{2}Z$ counts the captured polygons but subtracts half the captured short increasing paths.

Now fix two hemi-spheres, H and H' , and consider their *lune*, which is the closure of the points neither contained in H nor in H' ; see Figure 5. We are interested in the portion of the arrangement of great-circles in this lune. Each vertex of this portion lies either in the interior or on the boundary. For each interior vertex, we get two captured short increasing paths, and



■ **Figure 5** A lune identifies a portion of the arrangement of great-circles. Within this arrangement, we count polygons and short paths whose middle polygons are in the lune. We have two short increasing paths for each interior vertex and one for each boundary vertex, unless it is a corner of the lune, in which case we get no such path.

for each boundary vertex, we get one such path, except for the two corners of the lune for which we get no such path. Writing V_{int} and V_{bd} for the numbers of vertices in the interior and on the boundary, the number of captured short increasing paths is $2V_{int} + V_{bd} - 2$. The number of captured polygons is just the number of polygons in the lune, which we denote P . Ordering the lunes arbitrarily and writing X_i, Y_i, Z_i for the contributions of the lune defined by H and H' , we have

$$X_i = Y_i - \frac{1}{2}Z_i = P - \frac{1}{2}[2V_{int} + V_{bd} - 2]. \quad (49)$$

But $P = V_{int} + \frac{1}{2}V_{bd}$, which is easy to prove by adding the great-circles one at a time and counting how many vertices and polygons a great-circle adds to the portion of the arrangement in the lune. Hence $X_i = 1$. This implies $X = \sum_i X_i = \binom{n-2}{2}$ and therefore $\sum_{k=1}^{n-1} N_k = 1 + \binom{n}{2}$, as required. ◀

5 Discussion

The main contributions of this paper are an extension of the inductive argument for counting cells in order- k Voronoi tessellations from 2 to 3 dimensions, and the Morse theoretic perspective in which the number of cells are interpreted as alternating sums of critical polygons of 2-dimensional discrete Morse functions. Alternatively, we can state the results in terms of k -sets of n points on the unit 3-sphere or, more generally, for n points in convex position in \mathbb{R}^4 . There are connections between the alternating sums and the persistent homology of the discrete Morse functions, which may be interesting to develop in the future. There are a number of open questions this work raises:

- Can the Morse theoretic interpretation of higher order Voronoi tessellations be used to prove new upper and lower bounds on the maximum size of the order- k Voronoi tessellation of n points in \mathbb{R}^3 ? In particular, can we prove an upper bound asymptotically smaller than k^2n^2 or a lower bound asymptotically larger than k^2n ; see [2, 7]?
- Can the inductive approach be generalized to sets beyond 3 dimensions? Clearly yes, but how much more complicated does it get? Can we still hope for relations that involve only one independent variable, like N_k in \mathbb{R}^3 , or do we get extra independent variables?
- The regions in the order- k Voronoi tessellation correspond to k -sets of points on a sphere in \mathbb{R}^4 . Can the inductive approach be extended to points not necessarily in convex position? Proving bounds on the maximum number of k -sets in this more general setting is a notoriously difficult combinatorial problem, and any advance would be exciting [9].

References

- 1 Thomas Banchoff. Critical points and curvature for embedded polyhedra. *Journal of Differential Geometry*, 1:245–256, 1967.
- 2 Kenneth L. Clarkson and Peter W. Shor. Applications of random sampling in computational geometry, II. *Discrete & Computational Geometry*, 4:387–421, 1989.
- 3 Herbert Edelsbrunner and Georg Osang. A simple algorithm for higher-order Delaunay mosaics and alpha shapes. *Journal of Geometry*, 2021. (accepted).
- 4 Gábor Fejes Tóth. Multiple packing and covering of the plane with circles. *Acta Mathematica Academiae Scientiarum Hungaricae*, 27:135–140, 1976.
- 5 Robin Forman. Morse theory for cell complexes. *Advances in Mathematics*, 134(1):90–145, 1998.
- 6 Der-Tsai Lee. On k -nearest neighbor Voronoi diagrams in the plane. *IEEE Transactions on Computers*, 31(6):478–487, 1982.
- 7 Ketan Mulmuley. Output sensitive construction of levels and Voronoi diagrams in R^d of order 1 to k . In *Proceedings of the 22nd Annual ACM Symposium on Theory of Computing*, STOC'90, pages 322–330, 1990.
- 8 Michael I. Shamos and Dan Hoey. Closest-point problems. In *Proceedings of the 16th Annual Symposium on Foundations of Computer Science*, SFCS'75, pages 151–162, 1975.
- 9 Micha Sharir, Shakhur Smorodinsky, and Gábor Tardos. An improved bound for k -sets in three dimensions. *Discrete & Computational Geometry*, 26:195–204, 2001.
- 10 Georges Voronoi. Nouvelles applications des paramètres continus à la théorie des formes quadratiques. Deuxième mémoire: recherches sur les paralléloèdres primitifs. *Journal für die reine und angewandte Mathematik*, 134:198–287, 1908.